

CHAPTER 2 LITERATURE REVIEW

Introduction of Spark Plasma Sintering

Since 1990s[16], spark plasma sintering (SPS), also known as plasma activated sintering (PAS)[17] or field assisted sintering technique (FAST)[18], has become a popular sintering method for consolidation of powders in various fields[19]. As for a comparatively novel technique for sintering, SPS provides the possibility to sinter the material with better properties than conventional sintering methods and is capable of sintering what cannot be sintered in conventional methods[20]. Using the SPS, the finer grain sizes as well as the higher density can be achieved with the rapid heating rate. With such incredible features, great attentions have been drawn on SPS for both laboratory and industry applications. Figure 2-1 reveals the publications (on the left) and citations (on the right) of SPS listed from 1995 to 2014 in web of knowledge® citation index website. It is shown that within the past 18 years, the number of the publication has grown tremendous from 2 to more than 550 per year. And more than 7000 citations are recorded by the end of 2013. This rapid growing numbers of paper indicates the popularity of SPS among the scientific researchers. In industry, there are three major vendors supplying commercial SPS systems as listed in Table 2-1. Among them, there are at least two major vendors of SPS that have disclosed their ambition of making SPS system[21] that is capable of manufacturing massive products, large-size sample, near-net-shape sample with complex shape[22] as seen in Figure 2-2. All of these indicate a high demand of SPS in the industrial world.

The sintering mechanism in SPS is similar to the hot pressing and the green body is located in the graphite die with the uniaxial pressure applied to the powder using the graphite punch, as shown in Figure 2-3. Distinctively, instead of using external heating method, there is

pulsed direct current (DC), flows through the punches as well as the die, which means that the powders is heated from both outside and inside through Joule heating if the sample is electronically conductive. With the addition of the vacuum system, the whole set can provide the sinter period within 5 to 20 minutes and the sintering temperature 200 to 500 °C lower than the conventional counterparts, hot pressing.[23] Thus, it is of great importance for us to understand the intrinsic mechanism of SPS.

Mechanism Development of Spark Plasma Sintering

The mechanism of SPS was first described by M. Tokita[24] in 1993. In his paper, he introduced four major effects caused by large current pulse that result in the sintering characteristics, that is, spark plasma, spark impact pressure, Joule heating, and the electrical field diffusion effect. To illustrate all these effect, how the pulse current flows through the particles in SPS is schematized in Figure 2-4.

As shown in the figure, firstly, the powder surface are more easily purified and activated by passing the current through the die and powder particles directly, the Joule heat is then generated by the current, say I^2R , where I is the current flowing through the powder and R is the resistance of the powder. With the application of pressure, the high heating rate can be achieved due to the enhanced plastic flow of the powder. Secondly, the sintering stages in SPS includes the initial stage of spark discharging, generation of spark plasma and the vaporization and melting actions on the particle surfaces. Spark plasma generated the high temperature distribution and spark impact pressure eliminates the impurities on the particles surface. Then, high speed diffusion migration of ionized particles occurred under the electric field, and under the function of the pressure, the neck formed between the particles, following the conventional material transfer paths of sintering.

However, M. Tokita didn't provide the evidence to prove the mechanism he claimed. Mamoru Omori[25] used SPS for the etching of organic fibers to claim the existence of plasma. In the experiment, discharge is applied to the fibers in the graphite die for 3s with the atmosphere choosing from air, N₂, Ar, and vacuum. The SEM images of the discharged fibers are displayed in Figure 2-5. By contrast, the points on the surface of the polyethylene implied the generation of the plasma and the etched areas are localized. The points where spark plasma is generated are near the place of contacting other particles and there is no new bonds made in the process that connects fibers. By illustrating, he said that it is seemingly low energy plasma occurred with the energy higher than ultraviolet in the sintering by providing evidences that plasma cuts C-C bonds without generating carbon. [26]

In the research of Joanna R. Groza[27], the plasma hypothesis is proved by electrical discharge effects. She advocated that whereas the discharge hasn't been completely disclosed, distinct surface effects of the current discharges have been noticed in FAST consolidated specimens in YBCO. And by sintering the AlN alloy and Si₃N₄ powder[28], she also directly observed the clean grain boundaries with direct grain to grain contact and concentrated Al₂O₃ pockets in AlN, see Figure 2-6, and she claimed that either a low-temperature gas plasma state or a contact point plasma may be created by "micro-discharges" at the contact points of powder particles and there is critical voltage for the plasma generation. The effect of the plasma cleaning particle surface is also investigated[29] by K.R. Anderson and Groza. The transmission electron microscopy (TEM) observation of the FAST sintered NiAl shows that there are no surface oxide layers and the high and atomic resolution electron microscopy (HREM/ARM) of the pure tungsten powder indicated the clean boundaries, both of which implied the cleaning function of the pulsed electrical filed.

Meanwhile, some researchers disagree with the concept of plasma formation in the pulsed discharge sintering process. Dustin M. Hulbert [30, 31] in UC-Davis conducted a series of experiments in SPS using several different powders e.g. Al, Al₂O₃, NaCl, etc. to prove there is no plasma occurred during the sintering process. He adopted three major methods in his investigation:

1. In situ atomic emission spectroscopy
2. Direct visual observation
3. Ultrafast in situ voltage measurement.

In the spectroscopy, he claimed no characteristic photons were detected from the result. And due to the sensitivity issue of the AES device and human eyes and to make it more persuasive, he did the additional voltage measurement, and still, no voltage anomalies for the evidence of plasma were observed. Thus, none of the experimental methods employed detecting the generation of the plasma or any sparking or arcing present in the whole stages of SPS process.

While Dr Hulbert made the comprehensive experiments to exclude the plasma generated between the particles, it's still not safe to conclude that there are no plasmas since other factors that have not been well considered like the extent of the pressure and the size of the particles or there may occurs the arc in some small parts but not the whole sample that haven't been detected. Thus, it seems premature for Dr Hulbert's conclusion.

Apart from the direct discussion of the plasma generation, the researches turned to the current effect then. For the better understanding of role current played in the SPS, Umberto Anselmi-Tamburini's team composed a series of fundamental investigations. First, by studying the effect of DC pulsing on the reactivity[32] of Mo/Si system, he concluded that, the RMS(root mean square) of current value between the die is steady when changing the pulse pattern,

indicating RMS is the dominant condition to the power and temperature. In addition, direction has no effect on the reactivity as well as the different on-off pulse pattern. In the successive research, the modeling of current and heat distribution is established by utilizing the conductive and non-conductive materials as samples.[33] The current effect on the reactivity was studied and basing on the previous experimental data of SPS for Mo/Si system, he found that when under the current, MoSi₂ layer grows significantly faster than that without the current. And the presence of the current does not alter the original reaction mechanisms, [34]suggesting that the pulsing of DC, responsible for the activation of plasma, had no effect on the mass transport. For answering how the role of current on the mass transport, James M. Frei[35] sintered copper spheres to the copper plates by pulsed electric current method, see Figure 2-7. He said that volume diffusion mechanism is the dominant factor in absence of current on the neck growth. And under the current, the enhanced neck growth, see Figure 2-8, arises for the electro-migration with void formation in the high density areas of the current. In addition, the formation and increase in defect mobility under the influence of a current was also proved by Javier E. Garay [36] in his research on Ni₃Ti intermetallics, who indicated that changes in the concentration of point defects or mobility would result in the changes of growth mechanism.

As for the effect of the pressure to the rapid densification rate, J. Reis and R. Chaim[37] made effort by using a HIP model to construct the densification maps for SPS of nano-MgO. In this model, plastic yield and diffusion process are the dominating factors in the densification of SPS and factors of particle coarsening and grain growth are added to the HIP model as well. The result shows that the densification rates are too slow when applying HIP model to describe the SPS experimental data, which indicates the additional faster kinetics in densification mechanisms in SPS, implying the current effects. Chaim[38] also introduced the effect of the particle size in

SPS. The nano-sized particles may possibly activate discharge due to the narrow gap and high surface area. He claimed that, morphological and material dependently, nanoparticles enable high electric charge accumulating even under low voltages in SPS, which may result in the surface plasma formation and particle surface heating, the densification driving factors. The example is, when sintering yttrium aluminum garnet (YAG) under 360MPa at 1785 °C, which has the high yield stress in high temperature, the plastic deformation caused by the pressure cannot account for the rapid densification rate, see Figure 2-9, while the only reason is the nano size of the particles, on which the heated particle surface may become liquid and the liquid can aid for the grain rotation and sliding, accelerating the sintering process. Besides, Chaim and Zhijian Shen[39] also studied to control the grain size by external pressure application regime during SPS of YAG, concluding that applying pressure before significant coarsening of the particles in SPS is beneficial for the suppression of further grain growth in the densification process.

By using the numerical methods, Eugene A. Olevsky[23] considered two major factors of densification which contribute to SPS mass transfer: grain-boundary diffusion and power-law creep. In these material transport factors, three driving sources are considered: externally applied load, sintering stress (surface tension) and steady-state electro-migration while omitting a number of factors including possible plasma effect. From above, he derived the constitutive model and the densification map for aluminum, see Figure 2-10, using a series of equations for the total shrinkage rate in SPS by combining the grain-boundary diffusion and power-law creep mechanisms. Additionally, to broaden the scope of mechanisms in the modeling framework, he also studied the thermal factors[40, 41] in SPS that enhance the densification during SPS, and introduced the temperature gradient-driven thermal diffusion into account as well. By combining

the constitutive model to the shrinkage rate, the equation has been obtained and the result for the contributions of different mass transport mechanisms to the overall shrinkage rate are also calculated using the alumina powders, which is shown in the below figure 9 and which also corresponds well with the experimental data. In addition, the shape effect of the die in the role of SPS is also concerned now by Olevsky[42]. By considering the different geometry of the die, different thermal and electrical distribution would occur and the additional model should be established to comply with the growing demand of the industry.

Future and Challenge of Spark Plasma Sintering

Whereas it has shown clearly improvement from processing condition to final product in SPS, there are still some challenges preventing it from substituting conventional sintering methods. First, the problem of reduction and carbon contamination due to the low oxygen partial pressure in the SPS chamber causes side effects on the final product. It is documented in the literature that the properties of some sintered product are changed due to the carbon contamination [43, 44]. In our work, when sintering UO_2 at 1450°C in SPS, a thin layer of uranium carbide is detected which resulting in the crumbles of the resulting compact in most cases. Solving this problem may involve the improvement of the processing condition or changing the die materials. Noudem et al., [43] has managed to sinter the oxides under air atmosphere by using stainless steel/tungsten carbide dies. However, this modification can be only applied at low temperatures ($<1000^\circ\text{C}$). Alternative solution is yet to be developed for materials to sinter at high temperatures in SPS.

Another challenge for SPS is to fabricate large-scale, complicated-shape products. With the increase of the sample dimension, higher temperature gradient may occur within the sample. Also, the temperature distribution may become complicated when the complexity of the shape is increased. Both of them may have detrimental effect on the final product. As is mentioned in

[45], some efforts have been made to improve the situation. Additional heating element can be applied surrounding the die to decrease the temperature gradient. Also, a careful design of the die set makes it possible to sinter a relatively complex shape with identical microstructure [46].

Table 2-1. List of spark plasma sintering manufacturer

Manufacture	Max. Load[kN]	Max. Current[A]	Country	Reference
Sumitomo Coal Mining Company	50-3000	1000-20000	Japan	http://sps.fdc.co.jp/
Thermal Technology	100-2500	3000-60000	U.S	http://www.thermaltechnology.com/
FCT Systeme GmbH	50-4000	3000-48000	Europe	http://www.fct-systeme.de/

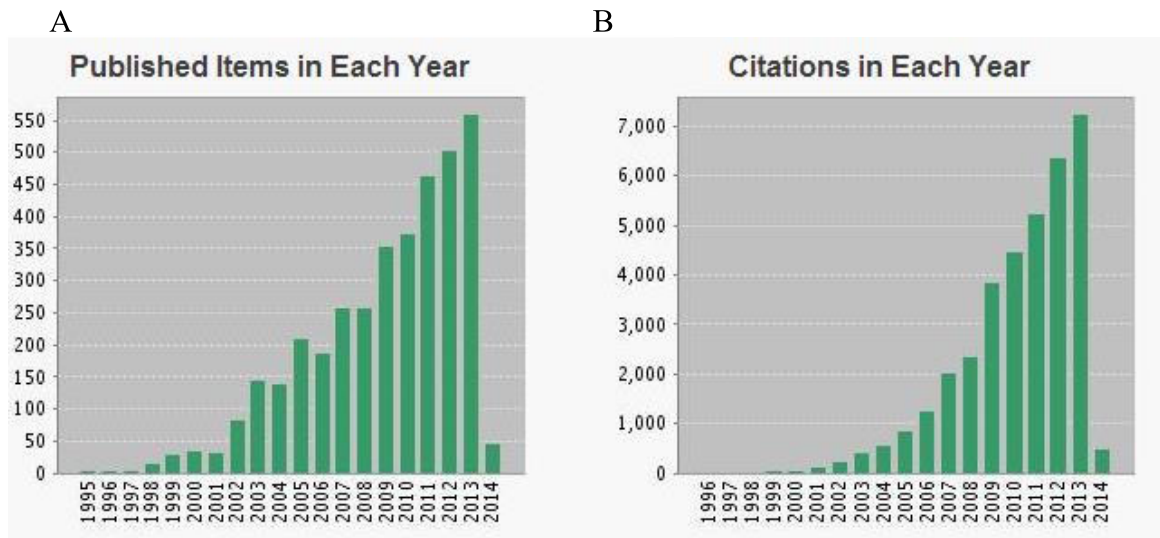


Figure 2-1. Scientific publication of SPS. A) Papers of SPS published from 1995 to 2014. B) Citations of SPS from 1995 to 2014.

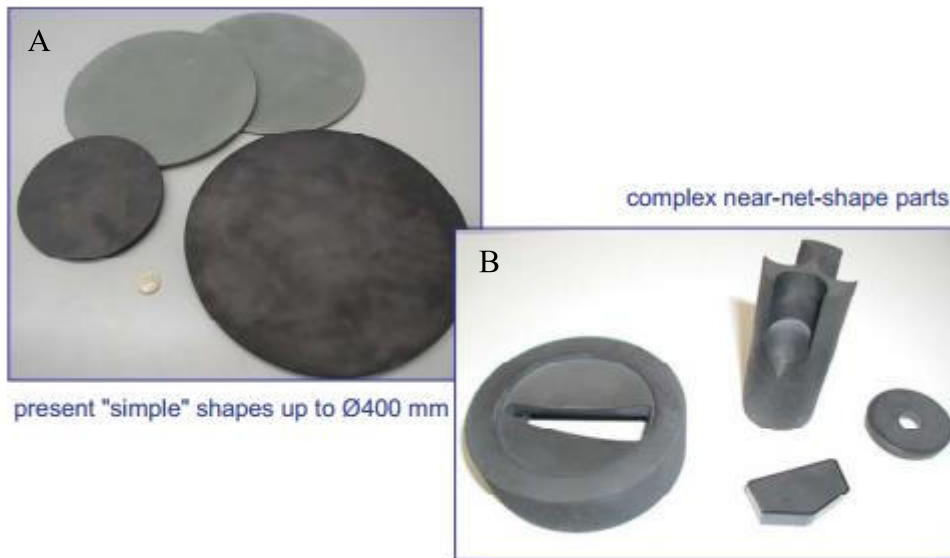


Figure 2-2. Sintered SPS Samples [22]. A) SPS sample with diameter up to 400 mm. B) Complex near-net shape parts.

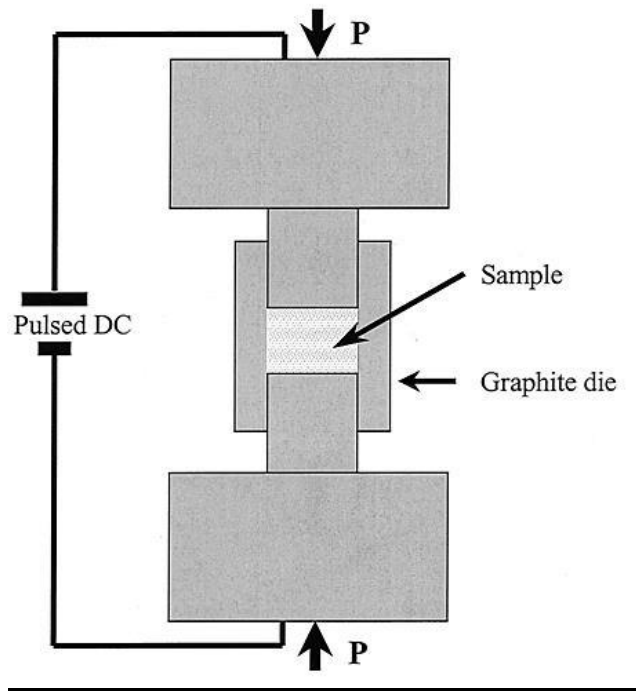


Figure 2-3. Schematic drawing illustrating the features of an SPS apparatus[47].

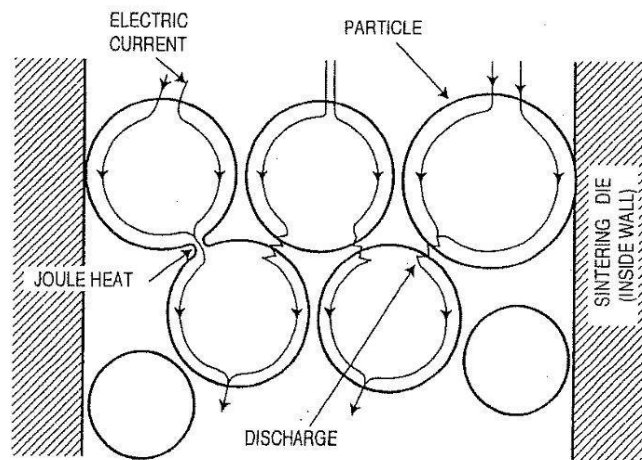


Figure 2-4. Effect of current on assisting densification of powder in SPS[16]

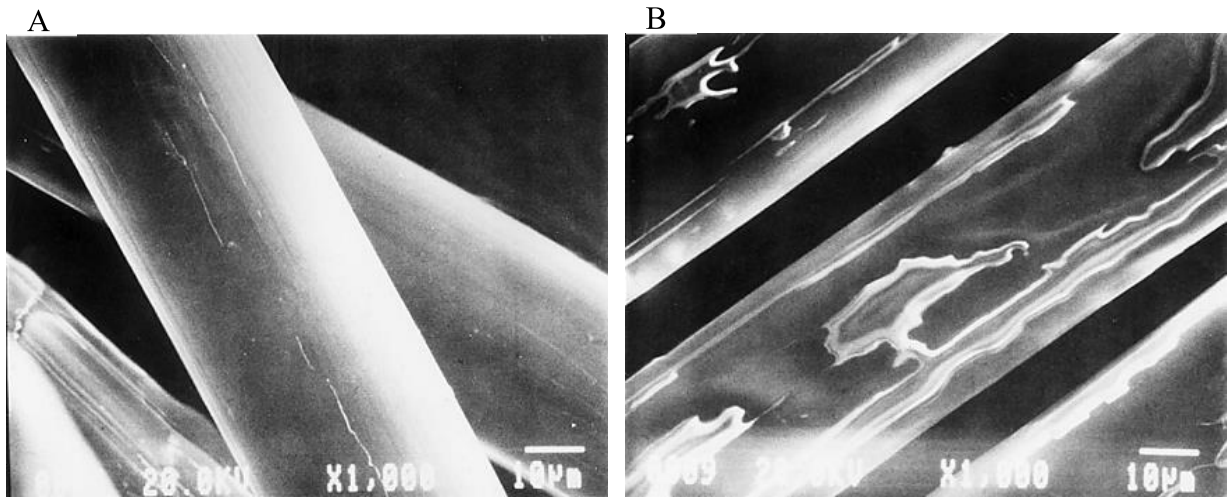


Figure 2-5. Image of polyethylene fiber revealing the effect of electrical discharge [25]. A) SEM image of polyethylene fiber. B) SEM image of the polyethylene fiber exposed to electrical discharge in air.

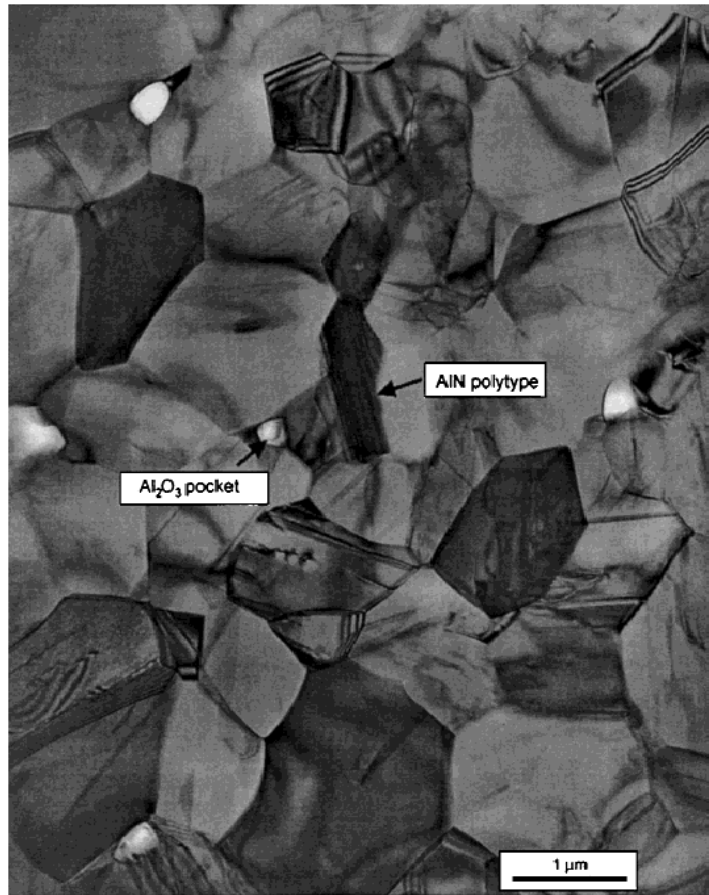


Figure 2-6. TEM micrograph of FAST-consolidated AlN. AlN polytypes and Al₂O₃ pockets are indicated by arrows [28].

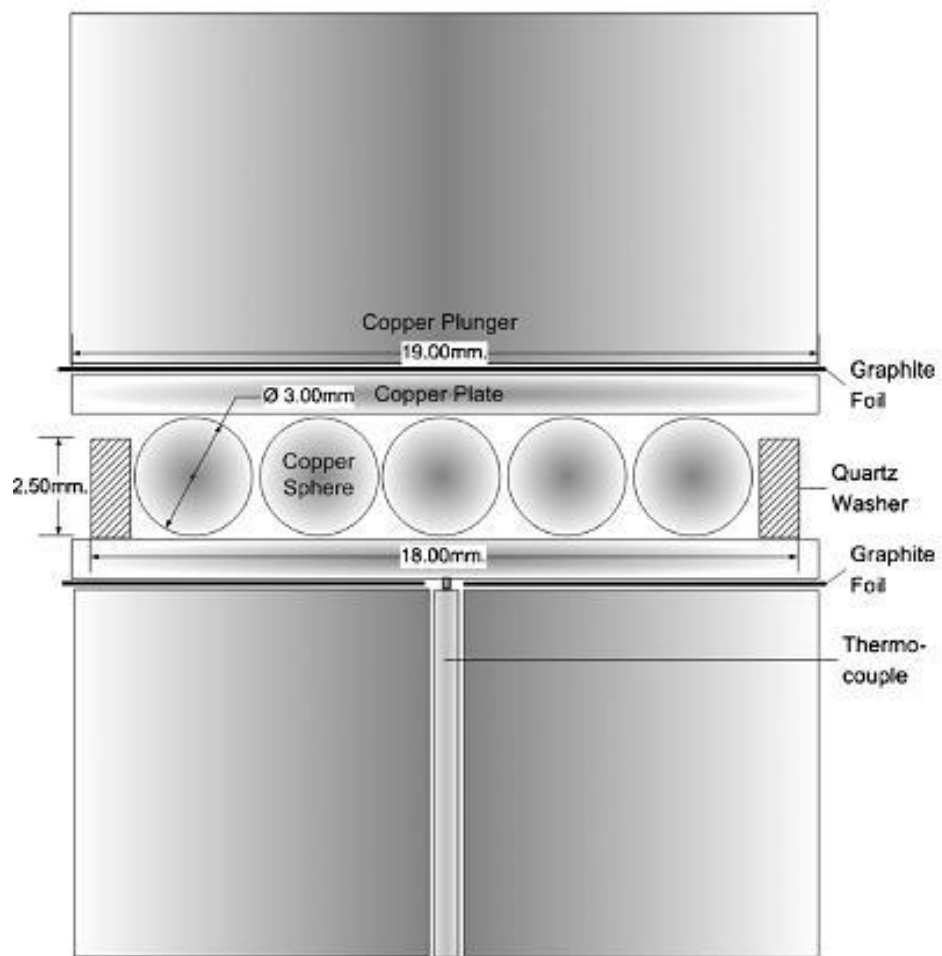


Figure 2-7. Schematic of sample of sphere to plate sintering geometry[48].

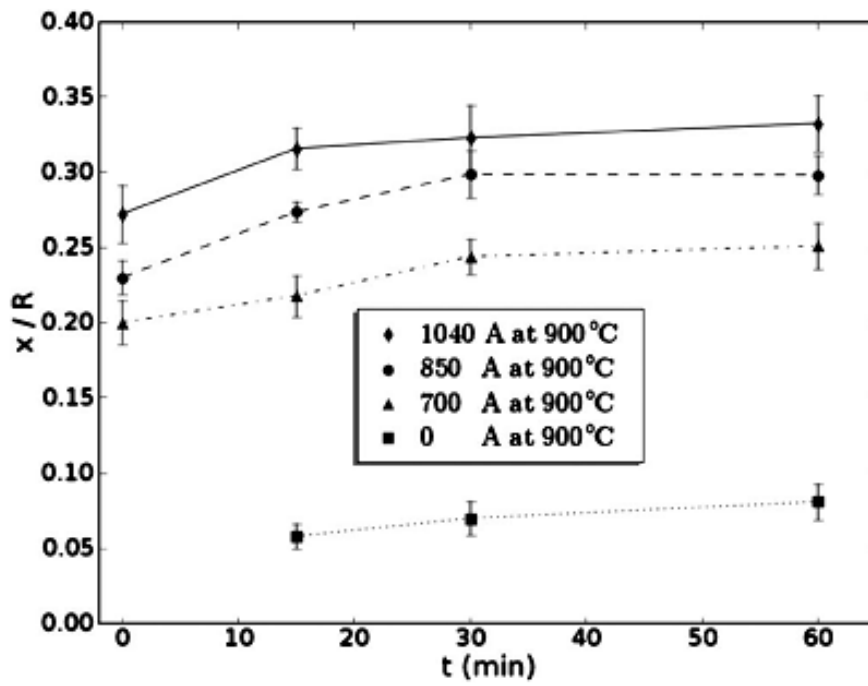


Figure 2-8. Time dependence of neck growth between copper spheres and copper plates at 900 °C under different currents. The neck size at zero time refers to the value obtained during ramp up to temperature[48].

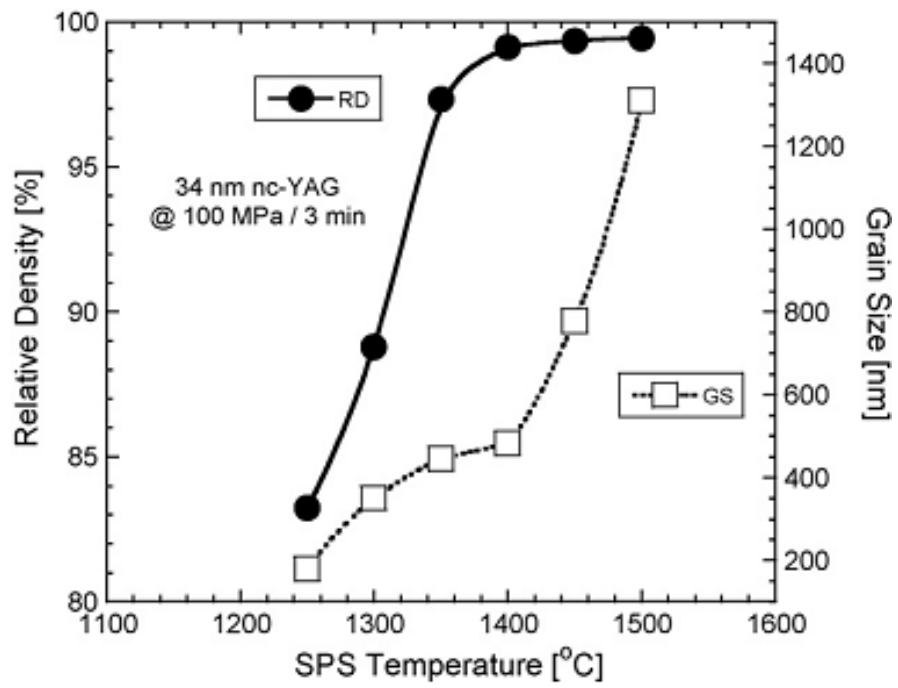


Figure 2-9. Relative density and grain size versus the SPS temperature of nc-YAG powder at 100MPa for 3min[38].

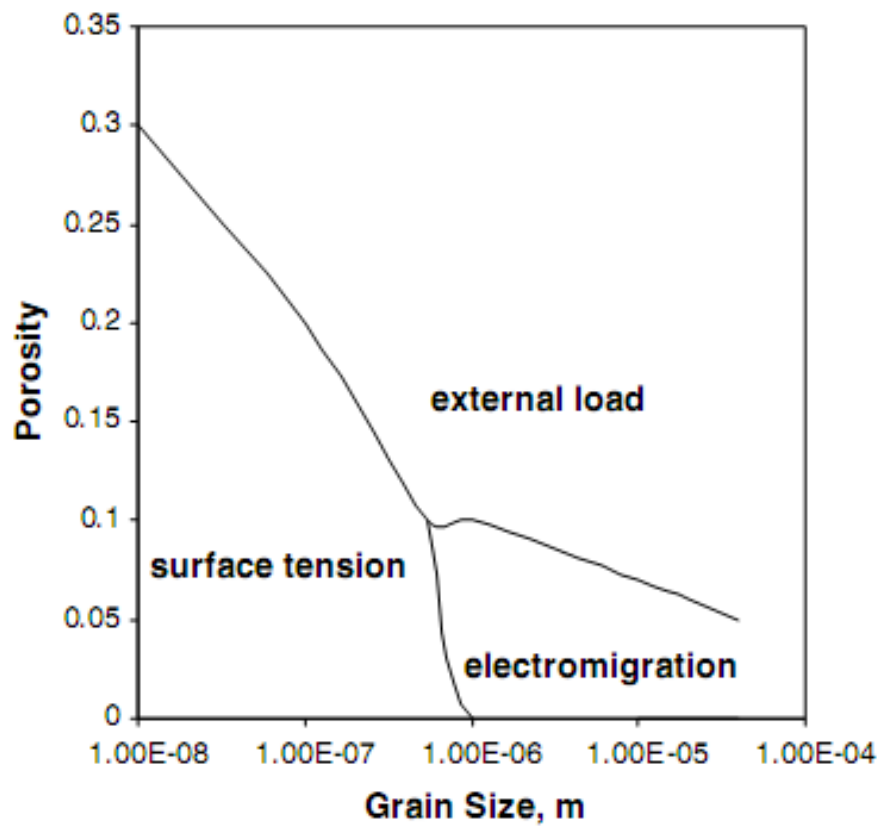


Figure 2-10. Densification map for aluminum powder in SPS, $T=673\text{K}$, Pressure= 2.83MPa [23]

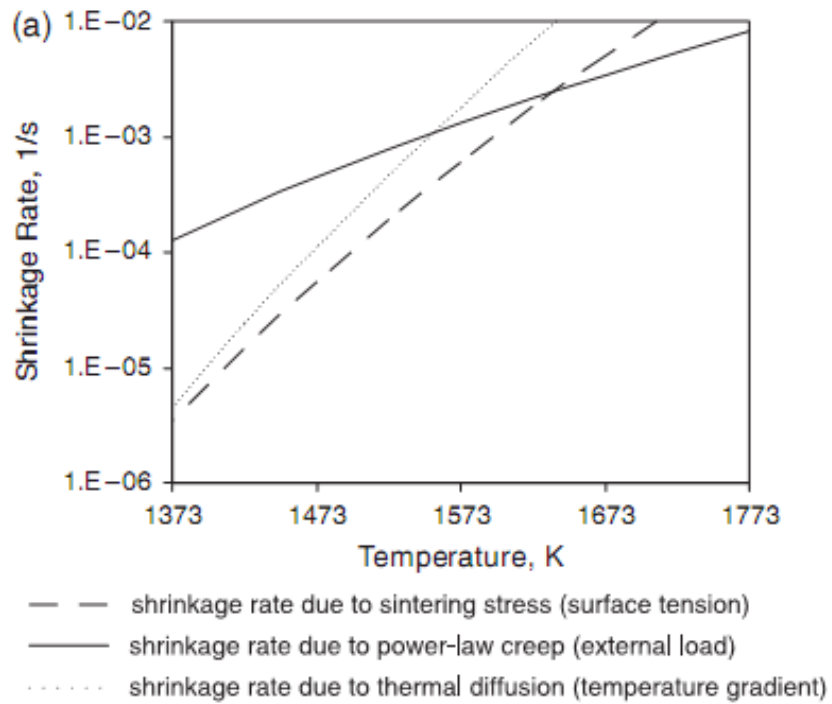


Figure 2-11. Contribution to shrinkage rate from different mechanisms of mass transport for an alumina powder, applied stress 30MPa, porosity 0.3 heating rate 200 K/min, grain size 0.5 μ m.[40]